Antiviral Research 165 (2019) 23–33

Contents lists available at ScienceDirect

Antiviral Research

journal homepage: www.elsevier.com/locate/antiviral

APOBEC3G is a restriction factor of EV71 and mediator of IMB-Z antiviral activity

Huiqiang Wang[a,b,1], Ming Zhong[a,b,1], Yanping Li[c], Ke Li[b], Shuo Wu[a,b], Tingting Guo[a,b], Shan Cen[c], Jiandong Jiang[a,b,**], Zhuorong Li[c,***], Yuhuan Li[a,b,*]

[a] Beijing Key Laboratory of Antimicrobial Agents, Institute of Medicinal Biotechnology, Chinese Academy of Medical Sciences and Peking Union Medical College, Beijing, China

[b] NHC Key Laboratory of Biotechnology of Antibiotics, Institute of Medicinal Biotechnology, Chinese Academy of Medical Science, Beijing, 100050, China

[c] CAMS Key Laboratory of Antiviral Drug Research, Institute of Medicinal Biotechnology, Chinese Academy of Medical Sciences and Peking Union Medical College, Beijing, China

ARTICLE INFO

Keywords:
APOBEC3G
Enterovirus 71
IMB-Z

ABSTRACT

Enterovirus 71 (EV71), a single-stranded positive-sense RNA virus, is the causative agent of hand, foot, and mouth disease (HFMD), for which no effective antiviral therapy is currently available. Apolipoprotein B messenger RNA-editing enzyme catalytic polypeptide-like 3G (APOBEC3G or A3G) is a cytidine deaminase that inhibits the replication of several viruses, such as human immunodeficiency virus-1, hepatitis B virus and hepatitis C virus. In our efforts toward understanding the antiviral spectrum and mechanism of A3G, we found that ectopic expression of A3G inhibited EV71 replication, whereas knockdown of endogenous A3G expression promoted EV71 replication. Moreover, inhibition of EV71 replication by IMB-Z, a *N*-phenylbenzamide derivative, is associated with increased levels of intracellular A3G, but reducing the level of A3G by RNA interference diminished the antiviral activity of IMB-Z. Mechanistically, we obtained evidence suggesting that the cytidine deaminase activity is not required for A3G inhibition of EV71 replication. Instead, we demonstrated that A3G can interact with viral 3D RNA-dependent RNA polymerase (RdRp) and viral RNA and be packaged into progeny virions to reduce its infectivity. Taken together, our results indicate that A3G is a cellular restriction factor of EV71 and mediator of the antiviral activity of IMB-Z. Pharmacological induction and/or stabilization of A3G is a potential therapeutic approach to treat diseases caused by EV71 infection, such as HFMD.

1. Introduction

Enterovirus 71 (EV71) is a single-stranded, positive-sense RNA virus belonging to the enterovirus genus of the *Picornaviridae* family. Although EV71 infection usually results in mild clinical symptoms and is self-limited, severe EV71 infection is often associated with neurological diseases, including aseptic meningitis, brain stem encephalitis, and acute flaccid paralysis (Wang et al., 2012a, 2017; Wu et al., 2013). EV71 infection also causes hand, foot, and mouth disease (HFMD) in children, mostly under 5 years of age. Since the first reported case of EV71 infection in California in 1969, EV71 outbreaks have been periodically reported worldwide, especially in the Asia-Pacific region (Cardosa et al., 2003; Chen et al., 2017; Huang et al., 2008; Wang et al., 2013). Hundreds of cases involving lethal complications have been reported in each outbreak. In China, EV71 caused a severe HFMD outbreak in 2008 and has now become a serious threat to children's health (Chen et al., 2017; He et al., 2017). Millions of children are infected with EV71 each year, and the morbidity and severity of HFMD have increased annually. However, no specific antiviral drug is currently available for treatment of EV71 infections.

APOBEC3G (apolipoprotein B messenger RNA [mRNA]-editing enzyme catalytic polypeptide-like 3G [A3G]), a member of the APOBEC superfamily, is an interferon-inducible cellular protein and plays an important role in defending viral infections. A3G is a cytidine

* Corresponding author. Beijing Key Laboratory of Antimicrobial Agents, Institute of Medicinal Biotechnology, Chinese Academy of Medical Sciences and Peking Union Medical College, Beijing, China.

** Corresponding author. Beijing Key Laboratory of Antimicrobial Agents, Institute of Medicinal Biotechnology, Chinese Academy of Medical Sciences and Peking Union Medical College, Beijing, China.

*** Corresponding author.

E-mail addresses: Jiang.jdong@163.com (J. Jiang), l-z-r@263.net (Z. Li), yuhuanlibj@126.com (Y. Li).

[1] These authors made equal contribution to the work.

https://doi.org/10.1016/j.antiviral.2019.03.005
Received 20 January 2019; Received in revised form 8 March 2019; Accepted 8 March 2019
Available online 09 March 2019
0166-3542/ © 2019 Elsevier B.V. All rights reserved.

deaminase containing a conserved His-X-Glu and Cys-X-X-Cys Zn^{2+} coordination motif and has been demonstrated to restrict the infection of several viruses, including human immunodeficiency virus-1 (HIV-1), T-cell leukemia virus type 1 (HTLV-1), hepatitis B virus (HBV) and hepatitis C virus (HCV) (Bishop et al., 2008; Chiu and Greene, 2008; Köck and Blum, 2008; Olson et al., 2018; Peng et al., 2011; Smith et al., 2012; Sasada et al., 2005; Zhu et al., 2015). Mechanistically, A3G inhibits retroviral replication by either cytidine deamination of viral DNA, which results in G-to-A hypermutation of viral genomes (Goila-Gaur and Strebel, 2008; Okada and Iwatani, 2016), or disruption of reverse transcription or genome encapsidation in a deaminase activity-independent manner (Fehrholz et al., 2012; Nguyen and Hu, 2008). However, A3G inhibition of HCV replication *via* interaction with viral NS3 protein in a deaminase activity independent manner (Zhu et al., 2015). Li et al. recently reported that A3G binds to the 5′UTR of EV71 to inhibit viral protein translation and genome replication. Intriguingly, EV71 antagonizes the restriction of A3G through its non-structural protein 2C that induces the autophagy–lysosome degradation of A3G (Li et al., 2018). Moreover, compound IMB-26 was reported to directly bind to and stabilize A3G (Cen et al., 2010). In our previous study, a series of *N*-phenylbenzamide derivatives of IMB-26 had been synthesized, and their anti-EV71 activities were assayed *in vitro* (Ji et al., 2013). Among the compounds tested, compound 5b (*N-(4-chlorophenyl)-4-methoxy- 3-propionamidobenzamide*, $C_{17}H_{17}N_2O_3Cl$, *MW* 332.78, Fig. 1A, renamed to IMB-Z) presented an improved antiviral activity against EV71 (Ji et al., 2013). In this study, we investigated the possibility that IMB-Z inhibition of EV71 replication is due to its elevation of cellular A3G.

2. Materials and methods

2.1. Cells and virus

African green monkey kidney (Vero) cells and human cervical cancer (H1-HeLa) cells were purchased from the American Type Culture Collection and cultured in Modified Eagle's Medium (Invitrogen, Carlsbad, CA, USA) supplemented with 10% inactivated fetal bovine serum (FBS; Gibco, Grand Island, USA) and 1% penicillin–streptomycin (Invitrogen, Carlsbad, CA, USA). Human embryonic kidney (293T) cells, human neuroblastoma (SK-N-SH) cells and human colon cancer (HCT-8) cells were purchased from the Cell Culture Center of Peking Union Medical College or Chinese Academy of Sciences and cultured in Dulbecco's Modified Eagle Medium (Invitrogen, Carlsbad, CA, USA) supplemented with 10% FBS and antibiotics (100 U/ml penicillin and 100 mg/ml streptomycin, Invitrogen) at 37 °C in a 5% CO_2 incubator.

EV71 strain H (VR-1432) and strain BrCr (VR-1775) were purchased from the American Type Culture Collection and propagated in Vero cells.

2.2. Compounds

IMB-Z was synthesized in the Medicinal Chemistry Laboratory of the Institute of Medicinal Biotechnology, Chinese Academy of Medical Sciences, with purity over 98.0%. The compound structure was confirmed with ^{1}H-NMR and MS spectra. 40 mM stock solutions of IMB-Z were prepared in dimethyl sulfoxide. IMB-Z was diluted to final working solutions as indicated in experiments.

2.3. Plasmids

EV71-VP1, VP2, VP3, VP4, 2B, 2C, 3A, 3C were constructed into pcDNA3.1 + vector with a HA tag at the carboxyl terminus by standard subcloning technology. pGFP-3B and pGFP-3D were kindly provided by Zhaohua Zhong, Department of Microbiology, Harbin Medical University. A3G was constructed into p3xFLAG-CMV vector or pCI-neo (pDMyc) vector by standard subcloning technology. The plasmids Flag-A3G (H257R), Flag-A3G (E259Q), and Flag-A3G (H257R & E259Q) were created by site-specific mutagenesis with Fast MultiSite Mutagenesis System (TransGen Biotech, Beijing, China) by following the manufacturer's direction.

2.4. Cytotoxicity assay

The cytotoxic effect of IMB-Z was assayed by Cell Counting Kit (CCK) (TransGen Biotech) (Wang et al., 2017).

2.5. Effects of exogenous A3G expression on EV71 replication

HCT-8 cells (4.0×10^5 cells per well of 6-well plate) were transfected for 24 h with plasmid Flag-A3G or p3xFLAG in Transln™ EL Transfection Reagent (TransGen Biotech). The culture media were removed, and cells were infected with EV71 (H, MOI = 0.1) for 1 h. Twenty-four hours later, the cells were harvested and total cellular proteins were extracted for Western blot assays.

2.6. RNA interference of A3G expression on EV71infection

HCT-8 cells were seeded into a six-well plate at 4.0×10^5 cells per well in complete growth medium. After 16 h of incubation, small interfering RNA (siRNA) (5′-CCAGGAAAUGGCUAAAUUCdTdT-3′ and 3′-dTdTGGUCCUUUACCGAUUUAAG-5′) (RiboBio, Guangzhou, China), that targets the sequence of A3G mRNA, were transfected into the cells by using Lipofectamine RNAiMAX (Invitrogen), with a nonrelevant control siRNA (RiboBio) as a control. The cells were infected with EV71 (H, MOI = 0.01) for 1 h at 48 h after siRNA transfection and harvested at 24 h post infection. Total cellular proteins were extracted for Western blot assays.

2.7. Effects of A3G expression on antiviral activity of IMB-Z against EV71

HCT-8 cells were seeded into six-well plates at a density of 4.0×10^5 cells/well. After 16 h of incubation, the cells were transfected with 1 μg of Flag-A3G or 25 nM of A3G RNAi and infected with EV71 (H, MOI = 0.1) at 24 h post transfection for 1 h. The infected cells were mock-treated or treated with IMB-Z (10 μM) immediately after viral inoculation for 24 h. The cells were harvested and total cellular proteins were extracted for Western blot assays.

2.8. Purification of EV71 virions

HCT-8 cells were seeded into 75 cm^2 culture flasks. After 16 h of incubation, the cells were infected with EV71 (H, MOI = 0.1) for 1 h and then treated with IMB-Z or solvent control. After treatment for 48 h, 35 ml of culture medium from EV71-infected cells was collected and cell debries were removed by centrifugation at 3200*g* for 15 min and 10,000 g for 20 min at 4 °C. The supernatant was filtered through a 0.22 μm membrane and further concentrated with Amicon Ultra-15 Centrifugal Filter Units (Millipore, Billerica, MA, USA). The concentrated virus preparations were placed onto a 20%–60% linear sucrose gradient and centrifuged at 125,000 g for 16 h at 4 °C. The upper layer of 20%–60% linear sucrose was completely removed and EV71 pellets at the bottom were collected and the EV71 and A3G proteins in the EV71 viral particles were detected by Western blot assays and immunoprecipitation.

2.9. Effects of IMB-Z on viral RNA hypermutation

The HCT-8 cells were seeded into 75 cm^2 culture flasks. After 16 h of incubation, the cells were infected with EV71 (BrCr, MOI = 0.1) for 1 h and then treated with IMB-Z or solvent control for 48 h. EV71 virions were purified as described above. HCT-8 cells were then infected with the purified EV71 virions and intracellular RNA were extracted at 6 h

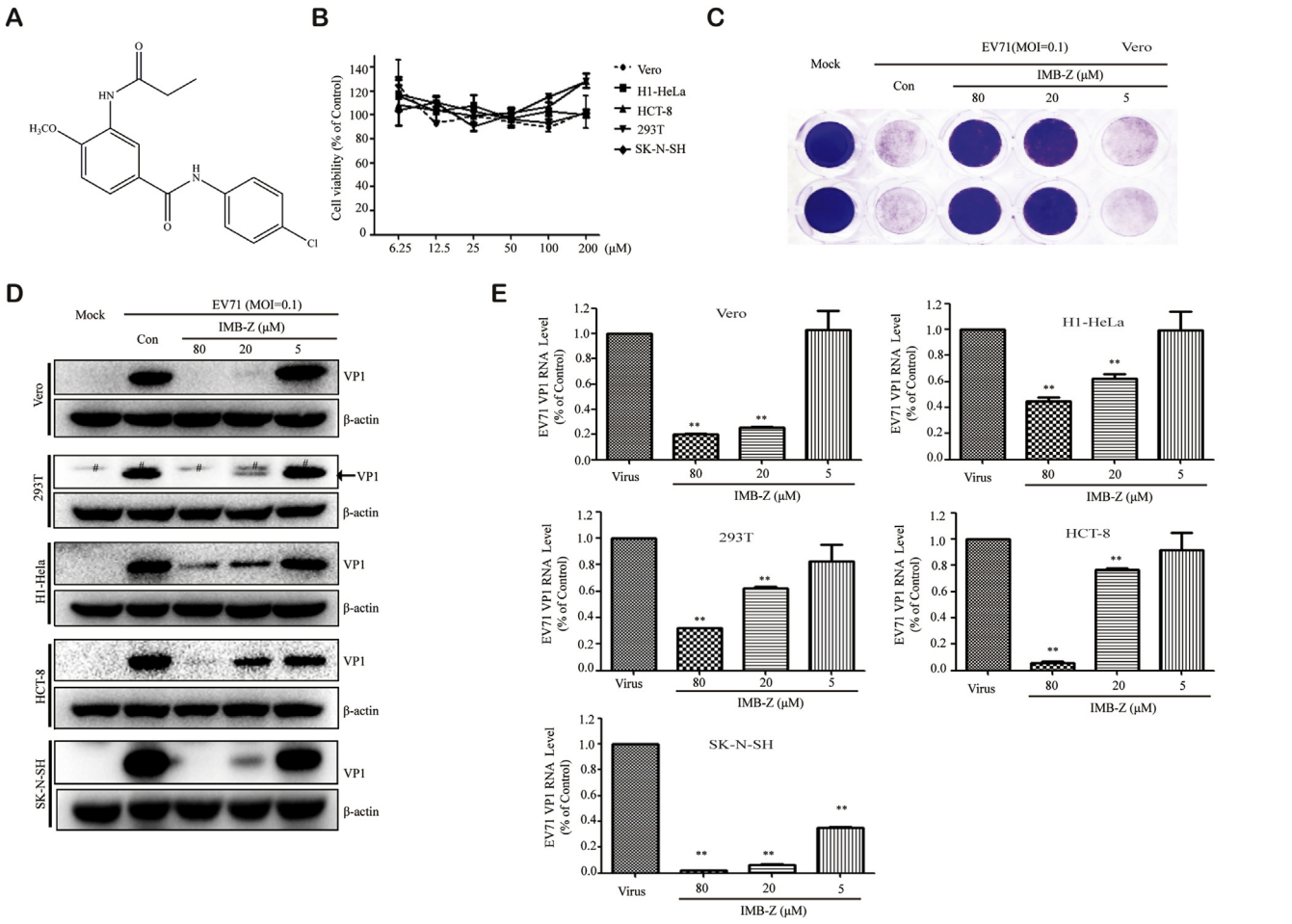

(caption on next page)

Fig. 1. IMB-Z inhibited EV71 replication in multiple cell types. (A) The chemical structure of IMB-Z. (B) Cytotoxicity of IMB-Z to multiple cell lines were determined by CCK assay. (C) Effects of IMB-Z on EV71-induced CPE in Vero cells were determined by crystal violet staining. (D and E) Cells (9×10^5 cells/well) were plated into 6-well culture plates and infected with EV71 (H, MOI = 0.1) for 1 h. The infected cells were then treated with the indicated concentrations of IMB-Z for 24 h. Intracellular viral VP1 protein (D) and RNA (E) were determined by Western blot and qRT-PCR assays, respectively. $^{**}P < 0.01$, $^{*}P < 0.05$ and $^{\#}$ for nonspecific band. (F) EV71 infected HCT-8 cells were revealed by immunofluorescent detection of VP1 protein using a fluorescence microscopy (×100).

post infection with the RNeasy Mini Kit (Qiagen, Germantown, MD, USA). EV71 RNA (2C) was amplified with the sense primer 5′-CGCGG ATCCAGTGCCTCATGGCTAAAG-3′ and antisense primer 5′-CCGGAAT TCTTATTGAAAGAGTGCTTCTATAGTATT-3′. The PCR products were purified with EasyPure™ Quick Gel Extraction Kit (TransGen Biotech) and inserted into the pEASY™-T1 Cloning vector (TransGen Biotech). The conjunct vector was transfected into the Trans 1-T1 Phage Resistant Chemically Competent Cell (TransGen Biotech) and cultured in Luria broth solid culture media (Invitrogen) with 100 μg/ml ampicillin. Individual colonies were picked up and amplified. The plasmids were extracted with the QIAprep Spin Miniprep Kit (Qiagen) and sequenced by Invitrogen Trading (Shanghai) Co., Ltd (Invitrogen, Shanghai, China).

2.10. Immunoprecipitation

293T cells were seeded into 75 cm^2 culture flasks. After 16 h of incubation, cells were transfected with plasmids encoding HA-VP1, HA-VP2, HA-VP3, HA-VP4, HA-2B, HA-2C, HA-3A, GFP-3B, HA-3C, or GFP-3D with Myc-A3G, Flag-A3G, Flag-A3G (H257R), Flag-A3G (E259Q), or Flag-A3G (H257R & E259Q). Cells were harvested at 48 h post transfection. Co-immunoprecipitation experiment was performed. Briefly, cells were collected and lysed using M-PER Mammalian Protein Extraction Reagent (Thermo Fisher Scientific, Waltham, MA, USA) containing halt protease inhibitor single-use cocktail (Thermo) for 30 min on ice. Soluble lysates were incubated with HA-Tag (Proteintech, Wuhan, China), GFP-Tag (Proteintech) and Myc-Tag (Proteintech) at 4 °C overnight, followed by incubation of protein A/G agarose beads (Roche, Basel, Switzerland) at 4 °C for 3 h. Complexes were separated from the beads and then boiled for 10 min. The precipitated proteins were subjected to SDS-PAGE and blotted with specific antibodies.

2.11. Real-time qRT-PCR

Total RNA was isolated from cells using the RNeasy Mini Kit and analyzed with the SuperScript III Platinum SYBR Green One-Step qRT-PCR Kit (Invitrogen). The RNAs of VP1, and actin were amplified by qRT-PCR with specific primers (Table 1) (Wang et al., 2017).

2.12. Western blot assay

Total cellular proteins were extracted using M-PER Mammalian Protein Extraction Reagent (Thermo) containing halt protease inhibitor single-use cocktail (Thermo). The extracted total protein or viral lysates were denatured by adding 5× sodium dodecyl sulfate–polyacrylamide gel electrophoresis (SDS-PAGE) sample buffer (Thermo), followed by boiling for 5 min at 100 °C. Approximately 15 μg proteins was applied for SDS-PAGE (Wang et al., 2017). The primary antibodies used in this study included antibodies against β-actin (Cell Signaling Technology, Beverly, MA, USA), EV71 VP1 (Abnova, Taipei, China), EV71-3AB (GeneTex, California, USA), EV71-2B (GeneTex), EV71-2C (GeneTex), EV71-3D (GeneTex), HA-Tag (Cell Signaling Technology), GFP-Tag (Cell Signaling Technology), Myc-Tag (Cell Signaling Technology) and A3G (Abcam, Cambridge, MA, USA). The goat anti-rabbit and anti-mouse HRP-labeled antibodies were obtained from Cell Signaling Technology.

Table 1
Quantitative real-time PCR primer sequences.

Primers	Nucleotide sequences (5'→3′)
EV71 VP1 forward	GATATCCCACATTCGGTGA
EV71 VP1 reverse	TAGGACACGCTCCATACTCAAG
β-actin forward	CACCATGTACCCTGGCATC
β-actin reverse	ACGGAGTACTTGCGCTCAG

2.13. Immunofluorescence assay

Vero cells grown on glass coverslips (Thermo) were infected with EV71 (H, MOI = 0.1) for 1 h. The infected cells were treated with the indicated concentrations of IMB-Z for 24 h and then fixed by 4% paraformaldehyde. The cells were permeabilized in 0.5% Triton X-100 at room temperature for 15 min and blocked in PBS containing 1% BSA for 1 h at room temperature. The cells were then incubated with an anti-EV71 VP1 antibody (Abnova) at a dilution of 1:500 for 2 h at room temperature. After washing three times with PBS, the samples were reacted with goat anti-mouse LgG and PE conjugate (TransGen Biotech) for 1 h at room temperature. After washing with PBS, the nucleus was detected with DAPI (Beyotime, Shanghai, China) and images were taken using a fluorescence microscope (Olympus, IX71, Japan).

2.14. Formaldehyde-crosslinked RNA-immunoprecipitation (RIP)

Three 10-cm plates of 95% confluent 293T cells were used for each sample. Cells were transfected with Myc-A3G and infected with EV71 (BrCr, MOI = 0.1) at 24 h post transfection for 1 h. The infected cells were left untreated or treated with 20 μM of IMB-Z for 24 h. Then, cells were crosslinked by adding phosphate buffered saline (PBS) containing 1% methanol-free formaldehyde and incubated for 10 min at 37 °C. Crosslinking was terminated by the addition of 2.5 M glycine to a final concentration of 0.125 M. Cells were washed three times with ice-cold PBS and scraped off the plates. RNA was extracted from an equal number of cells from each sample using the RNeasy Mini Kit (Qiagen). The remaining cells are centrifuged at 1000 × *g* for 3 min at 4 °C. Cell pellets were resuspended in 1 ml M-PER Mammalian Protein Extraction Reagent (Thermo) containing halt protease inhibitor single-use cocktail (Thermo) and 100U/ml R Nase inhibitor (TransGen Biotech). The lysates were centrifugated at 12,000 × *g* for 10 min, and the supernatant containing the protein-RNA complexes was subjected to IP overnight with an anti-Myc (Proteintech). On the following day, pre-blocked protein A/G agarose beads (Roche) were added to each sample for 3 h at 4 °C. The beads were then washed three times each with ice-cold PBS (100 U/ml RNase inhibitor). After proteinase K digestion, the RNA samples were extracted using the RNeasy Mini Kit (Qiagen) (Hao et al., 2018). The RNA of VP1 were amplified by qRT-PCR with specific primers the sense primer 5′- GATACCCTACATTTGGAGA -3′ and antisense primer 5′- TCGGGCATGCCCCATACTCGAG -3′. EV71 RNA (2C) was amplified by PCR with the sense primer 5′-CGCGGATCCAGTGCCTCA TGGCTAAAG-3′ and antisense primer 5′-CCGGAATTCTTATTGAAAGA GTGCTTCTATAGTATT-3.

2.15. Statistics

Data are expressed as the mean ± standard error of the mean. Two groups were compared by student's-test, more groups were compared by one-way ANOVA using MTLAB software (8.6, MathWorks, 2015; Natick, MA, USA) with $p < 0.01$ and $p < 0.05$ indicating statistical

significance.

3. Results

3.1. IMB-Z inhibits EV71 replication

In previous studies, we found that IMB-Z can prevent EV71-induced cytopathic effect (CPE) (Ji et al., 2013). To further determine the anti-EV71 activity of IMB-Z *in vitro*, we first determined the cytotoxicity of IMB-Z by CCK assay. The result showed that the maximum nontoxic concentration (TC_0) of IMB-Z was > 200 μM (Fig. 1B). At nontoxic concentrations, IMB-Z inhibited the CPE induced by EV71 infection in Vero cells, as revealed by crystal violet staining (Fig. 1C). As shown in Fig. 1D and E, IMB-Z treatment decreased the levels of viral VP1 protein and RNA in a dose-dependent manner in multiple different cell lines. Moreover, immunofluorescence assay also revealed that the number of VP1 positive cells was dose-dependently reduced in IMB-Z treated cultures (Fig. 1F). Those results convincingly demonstrated that IMB-Z inhibited EV71 replication in multiple cell types.

3.2. IMB-Z and EV71 infection regulate the level of intracellular A3G

It was reported previously that compound IMB-26 inhibited HIV-1 replication by specifically stabilizing A3G (Cen et al., 2010). As a derivative of IMB-26, we speculated that the antiviral effect of IMB-Z against EV71 may be due to modulating the steady-state level of A3G. Indeed, IMB-Z treatment increased the level of A3G protein in different cells in a time (Fig. 2A) and concentration (Fig. 2B) dependent manner. Interestingly, during the course of EV71 infection, the level of A3G in EV71 infected cultures increased at the early phase of infection (8 and 12 h), but declined in the later phase of infection (24 and 36 h) (Fig. 2C). However, IMB-Z treatment of EV-71 infected cells attenuated the late phase reduction of A3G and potently suppressed EV71 VP1 expression (Fig. 2D). Because A3G is an interferon-stimulated gene product, the increased expression of A3G in the early phase of infection could be a result of virus-induced interferon response, and the decreased expression of A3G at the late phase of infection might be due to A3G degradation induced by viral protein 2C (Li et al., 2018).

3.3. A3G is a host restriction factor of EV71

To investigate the role of A3G in EV71 infection, we examined the effects of modulating the intracellular levels of A3G on EV71 replication. We first demonstrated that ectopic expression of A3G in HCT-8 cells significantly reduced the levels of viral VP1 protein (Fig. 3A), whereas reducing A3G expression by siRNA interference in HCT-8 cells increased the level of VP1 protein (Fig. 3B). Interestingly, we also showed that combination of A3G ectopic expression and IMB-Z treatment more efficiently reduced the level of VP1 protein (Fig. 3C, comparing lanes 3 and 4 to lane 5) and RNA (Fig. 3D), but reducing the endogenous A3G by siRNA interference in HCT-8 cells attenuated IMB-Z-induced reduction of VP1 protein (Fig. 3E, comparing lane 3 to lane 5) and RNA (Fig. 3F). Moreover, in agreement with our previous report that IMB-26 stabilized A3G, IMB-Z treatment elevated the levels of A3G protein in HCT-8 cells transfected with plasmid expressing Flag-A3G (Fig. 3C, comparing lane 4 to lane 5) or siRNA targeting A3G mRNA (Fig. 3E, comparing lane 4 to lane 5). In summary, these results indicated that A3G is a host restriction factor of EV71 and IMB-Z inhibition of EV71 is through modulation of intracellular level of A3G.

3.4. Cytidine deaminase activity was not required for A3G to inhibit EV71replication

Concerning the antiviral mechanism of A3G, it is plausible to consider the potential role of deaminase activity in restriction of EV71 replication. To investigate this possibility, we first examined whether increasing the level of A3G in EV71 infected cells by IMB-Z treatment induces cytidine deamination of viral RNA. Accordingly, HCT-8 cells were infected with EV71 and treated with IMB-Z or solvent control for 48 h. EV71 virions were purified from culture media and used to infect naïve HCT-8 cells. At 6 h post infection, cells were harvested and total cellular RNA was extracted. The deaminase activity of A3G is highly sequence specific and the third position of a triplet cytosine (CCC) hotspot is converted into CCU. Because the coding region of 2C protein is relative conserved and has nine tripletcytosine, this region was amplified by RT-PCR and sequenced to determine the frequency of hypermutation. Compared to viral RNA derived from mock-treated cells, viral RNA derived from IMB-Z treated cells demonstrated a similar rate of G/A mutation (Table 2). This result implies that inhibition of EV71 replication by IMB-Z does not induce cytidine deamination-induced G-to-A hypermutation of viral RNA.

Moreover, it has been reported that two amino acid residues, H257 and E259, in C-terminal CD2 domain of A3G are critical for deaminase catalytic activity (Iwatani et al., 2006; Li et al., 2011; Navarro et al., 2005; Newman et al., 2005) (Fig. 4A). To rigorously determine the role of deaminase activity in inhibiting EV71 replication, 293T cells were transfected with control vector plasmid or plasmid expressing wild-type or deaminase-deficient A3G. The cells were then infected by EV71 and viral protein VP1 were examined by Western blot assay at 24 h post infection. As shown in Fig. 4B, ectopic expression of wild-type A3G or each of the three deaminase-deficient A3G demonstrated a similar activity of reducing viral VP1 protein expression.

3.5. EV71 3D protein interacts with A3G

It was reported previously that A3G inhibits viral replication by directly interacting with viral proteins, such as HCV non-structural protein NS3 (Zhu et al., 2015). To investigate whether A3G interacts with any of EV71 proteins, 293T cells were co-transfected with a plasmid expression Myc-tagged A3G and a vector plasmid or plasmid expressing HA-tagged VP1, VP2, VP3, VP4, 2B, 2C, 3A, 3C or GFP-tagged 3B, 3D protein. As shown in Fig. 5A, immunoprecipitation with antibody against Myc epitope tag and probing the precipitated viral proteins with antibodies against HA tag or GFP indicated that A3G protein does not interact with HA-tagged VP1, VP2, VP3, VP4, 2C, 3A, 3C protein or GFP-tagged 3B protein, but interacts with GFP-3D protein and HA-tagged 2B protein. To confirm the specificity of the interaction, we further demonstrated that Myc-A3G protein could also be pulled down by GFP-tagged 3D protein, but not HA-tagged 2B protein (Fig. 5B).

To investigate whether 3D interacts with A3G in the context of EV71 infection, 293T cells transfected with a plasmid expressing Myc-A3G were infected by EV71 and harvested at 24 h post infection. Immunoprecipitation from the cell lysates with anti-Myc antibody and probed with antibody against viral 3AB, 2B, 2C or 3D protein. As shown in Fig. 5C, the results showed that 3D, but not 3AB, 2B and 2C protein, was enriched in the precipitated immunocomplex (Fig. 5C). In addition, we used the antibody against A3G protein to do immunoprecipitation by EV71 infecting HCT-8 cells and used 3D antibody to do western blot to check the endogenous interaction between A3G and 3D. As shown in Fig. 5D, there is an endogenous interaction between A3G and 3D. Moreover, A3G with H257Q and/or E259Q substitution did not affect its interaction with 3D protein (Fig. 5E). These results convincingly demonstrated that A3G specifically interact with viral protein 3D in infected cells in a deaminase activity-independent manner.

3.6. IMB-Z treatment increases A3G encapsidation into progeny virions and reduces its infectivity

In addition to interact with viral proteins involving in genome replication, A3G has also been reported to be packaged into HBV or HCV viral particles (Nguyen and Hu, 2008; Zhu et al., 2015). To investigate

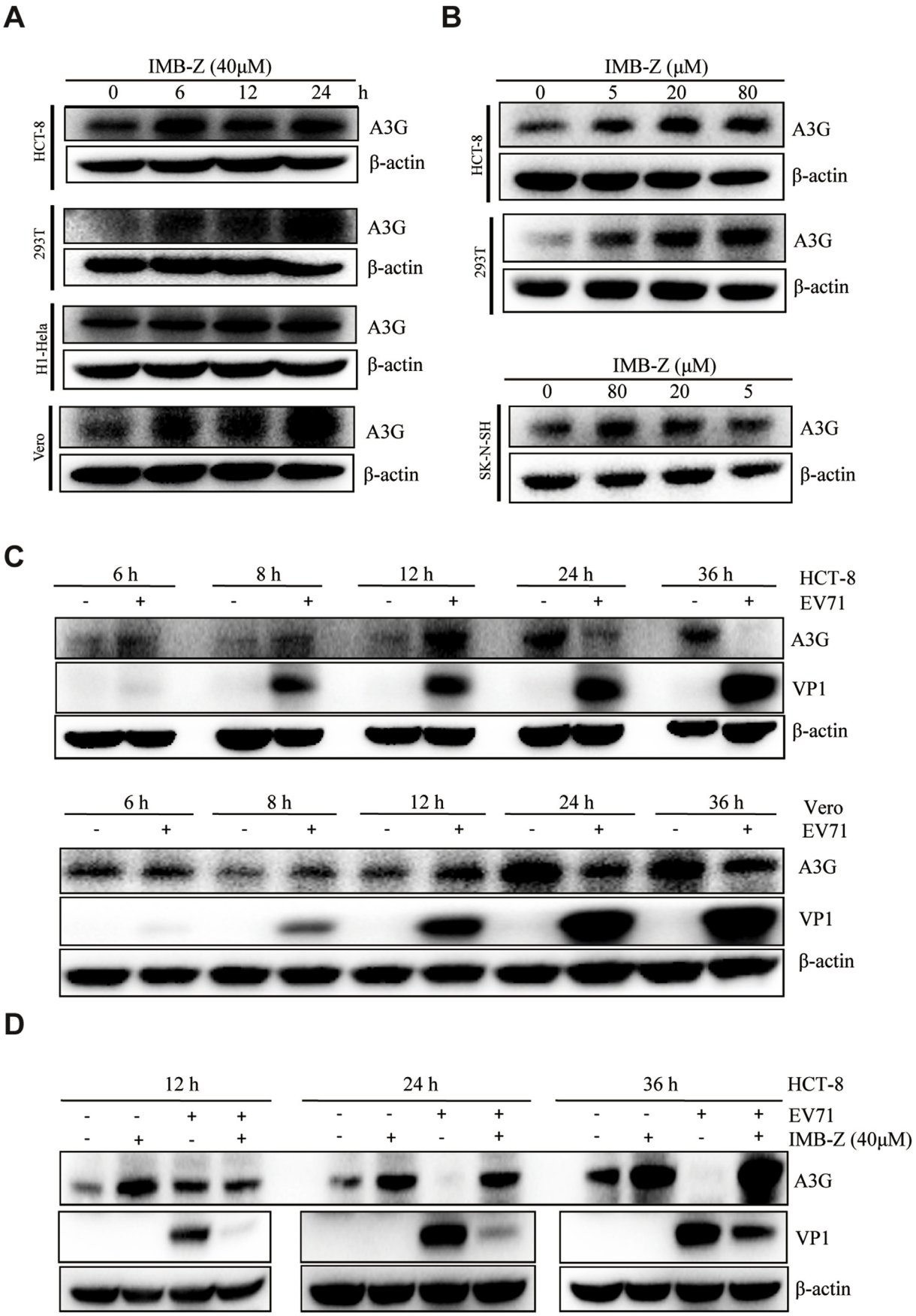

Fig. 2. Both IMB-Z treatment and EV71 infection increases the level of intracellular A3G. (A,B) Cells were treated with indicated concentrations of IMB-Z for the indicated period of time. (C) Cells were mock-infected (−) or infected with EV71 (H, MOI = 3) and harvested at the indicated time post infection. The amounts of viral (VP1) or cellular (A3G and β–actin) proteins were determined by Western blot assays. (D) Cells were infected with EV71 (H, MOI = 3) for 1 h. The infected cells were then treated with IMB-Z and harvested at the indicated time post infection for Western blot assays.

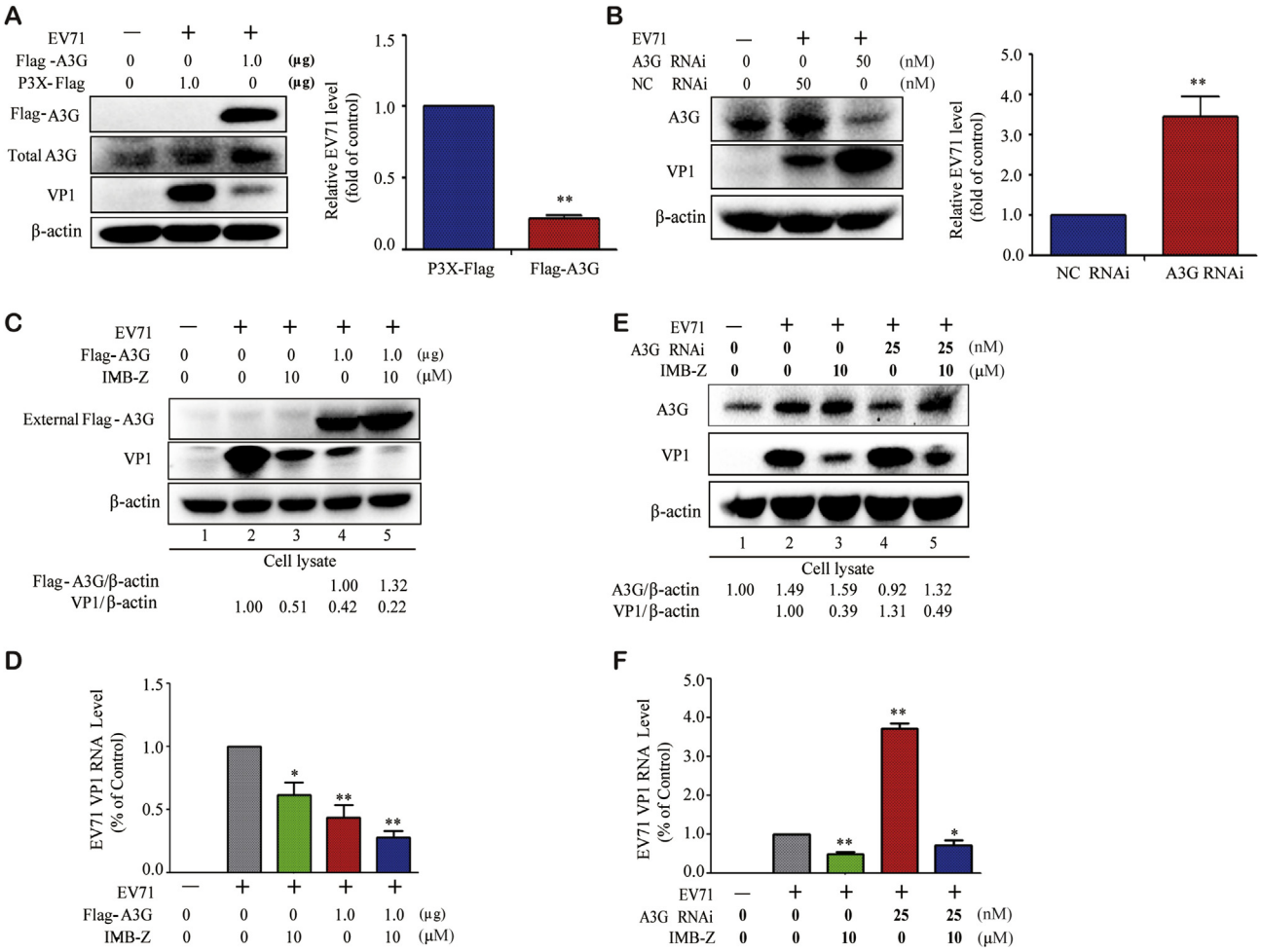

Fig. 3. A3G is a host restriction factor against EV71. (A, C and D) Ectopic expression of A3G reduced EV71 replication in the HCT-8 cells. To introduce A3G, HCT-8 cells were transfected with a plasmid expressing Flag-A3G or control vector P3X-Flag and infected with EV71 (H, MOI = 0.1) at 24 h post transfection for 1 h. The infected cells were left untreated or treated with 10 μM of IMB-Z for 24 h. Viral and cellular proteins were determined by Western blot and viral RNA was determined by qRT-PCR. (B, E and F) Silencing the endogenous A3G expression in HCT-8 cells increased EV71 replication. HCT-8 cells transfected with 25 nM siRNA specifically targeting A3G mRNA or control siRNA and infected with EV71 (H, MOI = 0.1) at 24 h post transfection for 1 h. The infected cells were left untreated or treated with 10 μM of IMB-Z for 24 h. Viral and cellular proteins were determined by Western blot assays and viral RNA was determined by qRT-PCR. The levels of VP1 and A3G proteins were quantified by software "Gel-Pro analyzer". *$P < 0.05$, **$P < 0.01$.

Table 2
Effect of IMB-Z on viral RNA hypermutations.

Samples	Total Bases	Total Mutations	Mutate Rate (‰)	G to A Mutations
11	Virus control	40426(986 × 41[a])	57	1.41
13	IMB-Z treated	40426(986 × 41[a])	50	1.24

[a] Total number of EV71 clones tested in the study.

if A3G could be packaged into EV71 progeny virions, HCT-8 cells infected with EV71 (H, MOI = 0.1) were cultured for two days in the presence or absence of IMB-Z. EV71 viral particles in the culture medium were concentrated by ultracentrifugation. The amounts of viral structure protein VP1 and genomic RNA in the virion preparations from mock-treated and IMB-Z-treated culture medium were determined. Equal amounts of virions, as normalized by VP1 protein, were resolved by SDS-PAGE and viral and cellular proteins were detected by Western blot assays. Compared with those from untreated cells, the A3G protein was significantly increased in the EV71 particles produced from the IMB-Z-treated HCT-8 cells (Fig. 6A, upper panel). To further confirm the encapsidation of A3G, equal amounts of virion preparations from mock-treated and IMB-Z-treated culture medium were subjected for immunoprecipitation with antibody against VP1. The immunoprecipitated VP1 and A3G proteins were detected by Western blot assay. The results (Fig. 6A, lower panel) showed that the virions produced from IMB-Z-treated cells encapsidate significantly more A3G molecules. Moreover, we were not able to detect exogenously expressed A3G in the virus particles (data not shown), which was consistent with the results of li et al. (Li et al., 2018).

Host proteins can be packaged into virions through interaction with viral structural proteins or genomic RNA. Although our study found that there is an interaction between A3G and 3D protein, since 3D protein is a non-structural protein, we speculated that the interaction between A3G and EV71 RNA might be responsible for A3G packaging into viral particles. Indeed, as shown in Fig. 6B and C, A3G did bind to EV71 RNA in infected cells as demonstrated by a formaldehyde-cross-linked RNA-immunoprecipitation (RIP) assay.

To investigate the effect of encapsidated A3G on virion infectivity, we compared the replication of progeny virions derived from mock treated or IMB-Z treated cultures. In this experiment, EV71-infected HCT-8 cells were cultured for two days in the presence or absence of IMB-Z. The resultant EV71 viral particles in the culture fluid were harvested by ultracentrifugation. Viral RNA in the viral particle

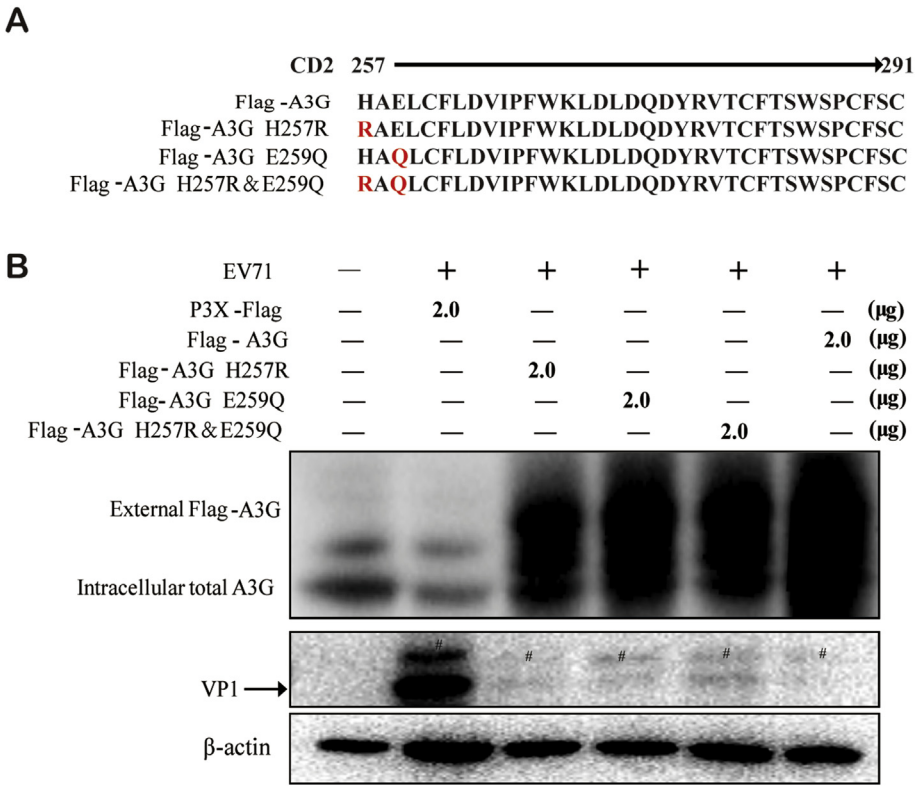

Fig. 4. Cytidine deaminase activity of A3G is not required for its inhibition of EV71 replication. (A) Amino acid residues critical for deaminase activity of A3G is highlighted. (B) 293T cells were transfected with 2 μg of plasmid expressing wild type or different mutant A3G. The cells were infected with EV71 (H, MOI = 0.1) at 24 h post transfection and harvested at 24 h post infection. The indicated viral and cellular proteins were detected by Western blot assays. An antibody against A3G, but not tag epitope, was used for detection of both endogenous and ectopically expressed A3G. # Non-specific band.

preparations were quantified by qRT-PCR. Vero cells were infected with equal genome-equivalent of EV71, and 50% tissue culture infective doses ($TCID_{50}$) was detected by using the CPE method. As shown in Fig. 6D, the progeny of EV71 prepared from IMB-Z treated HCT-8 cultures showed a significantly reduced $TCID_{50}$. This finding implies that IMB-Z increases the amount of A3G packaged into EV71 particles, which reduces the infectivity of progeny viruses.

4. Discussion

APOBEC3 family of antiviral proteins restricts viral infections *via* cytidine deaminase-dependent and independent mechanisms. A3G is the first APOBEC3 member identified as a host restriction factor of HIV-1 (Sheehy et al., 2002). Since then, A3G has been demonstrated to inhibit the replication of other retroviruses (HTLV-1), pararetrovirus (HBV) and RNA virus (HCV) (Albin and Harris, 2010; Kitamura et al., 2013; Komohara et al., 2006; Sasada et al., 2005). Herein, we obtained evidence showing that A3G inhibits the replication of a picornavirus, EV71.

The molecular mechanism underlying A3G restriction of HIV-1 infection had been extensively investigated. A3G protein is packaged into HIV-1 virions *via* interacting with Gag protein (Chelico et al., 2009). Upon infection of susceptible cells, A3G deaminates cytosines in the single-stranded complementary DNA reverse-transcribed from viral geniomic RNA and thus, introducing G-to-A mutations into positive-strand DNA (Goila-Gaur and Strebel, 2008). The G-to-A hypermutation is lethal or severely compromises viral protein expression and genome replication. In addition, A3G was also reported to interact with HIV-1 integrase, nucleocapsid or reverse transcriptase to inhibit viral DNA synthesis and proviral DNA formation (Luo et al., 2007; Wang et al., 2012b). Similarly, A3G inhibits the replication of HBV, a pararetrovirus, by inducing G-to-A hypermutation (Kitamura et al., 2013; Noguchi et al., 2005; Suspene et al., 2005) as well as inhibition of reverse transcriptional DNA synthesis in nucleocapsids. It was demonstrated that packaging of A3G into HBV nucleocapsids is dependent on the viral DNA polymerase and RNA packaging signal epsilon element of pregenomic (pg) RNA (Nguyen and Hu, 2008). However, A3G inhibits HCV replication by binding to viral NS3 protein at its C-terminus, which is responsible for NS3's helicase and NTPase activity (Zhu et al., 2015). Although A3G usually inhibits viral replication through cytidine deamination-induced G/A hypermutation of viral genomes, we obtained two independent lines of genetic evidence suggesting that deaminase activity is not required for A3G restriction of EV71 (Table 2 and Fig. 4). As a host restriction factor to many retroviruses and a few RNA viruses, viruses usually evolve distinct mechanisms to evade A3G restriction. For instance, HIV-1 Vif protein binds A3G and targets it for proteolytic degradation, whereas foamy virus Bet protein binds and prevents A3G to be packaged into virions (Conticello et al., 2003; Jaguva Vasudevan et al., 2013).

In this study, we found that EV71 infection could reduce the expression of A3G in the later phase of infection (Fig. 2B), which is consistent with the report by Li and colleagues that non-structural protein 2C antagonized A3G through induction of an autophagy–lysosome degradation (Li et al., 2018). However, we found that A3G specifically interacted with EV71 3D protein, but not 2C, in virally infected cells (Fig. 5). The reason for the discrepancy is currently not known. In addition, we were not able to detect exogenously expressed A3G in the virus particles, which was consistent with the results of li et al. (Li et al., 2018). However, we obtained evidence indicating that endogenously expressed cellular A3G can be packaged into progeny EV71 virions. It may be due to the difference between exogenous expression of A3G and endogenous A3G. Furthermore, treatment of the EV71 infected cells with IMB-Z compound resulted in secretion of virions with increased level of encapsidated A3G, which might thus be responsible for the reduced infectivity (Fig. 6). Using an RNA-immunoprecipitation assay, we showed that A3G could bind to viral RNA in infected cells (Fig. 6B). Li et al. also found that A3G could bind to the loop I and II of EV71 5′UTR *in vitro*. Therefore, it is possibly that packaging of A3G into viral particles might be mediated by its interaction with viral RNA, particularly its 5′UTR. Although the reason for the discrepancy between ours and Li's results, both studies clearly indicate that A3G restricts EV71 replication in a deaminase activity-independent manner. Our study

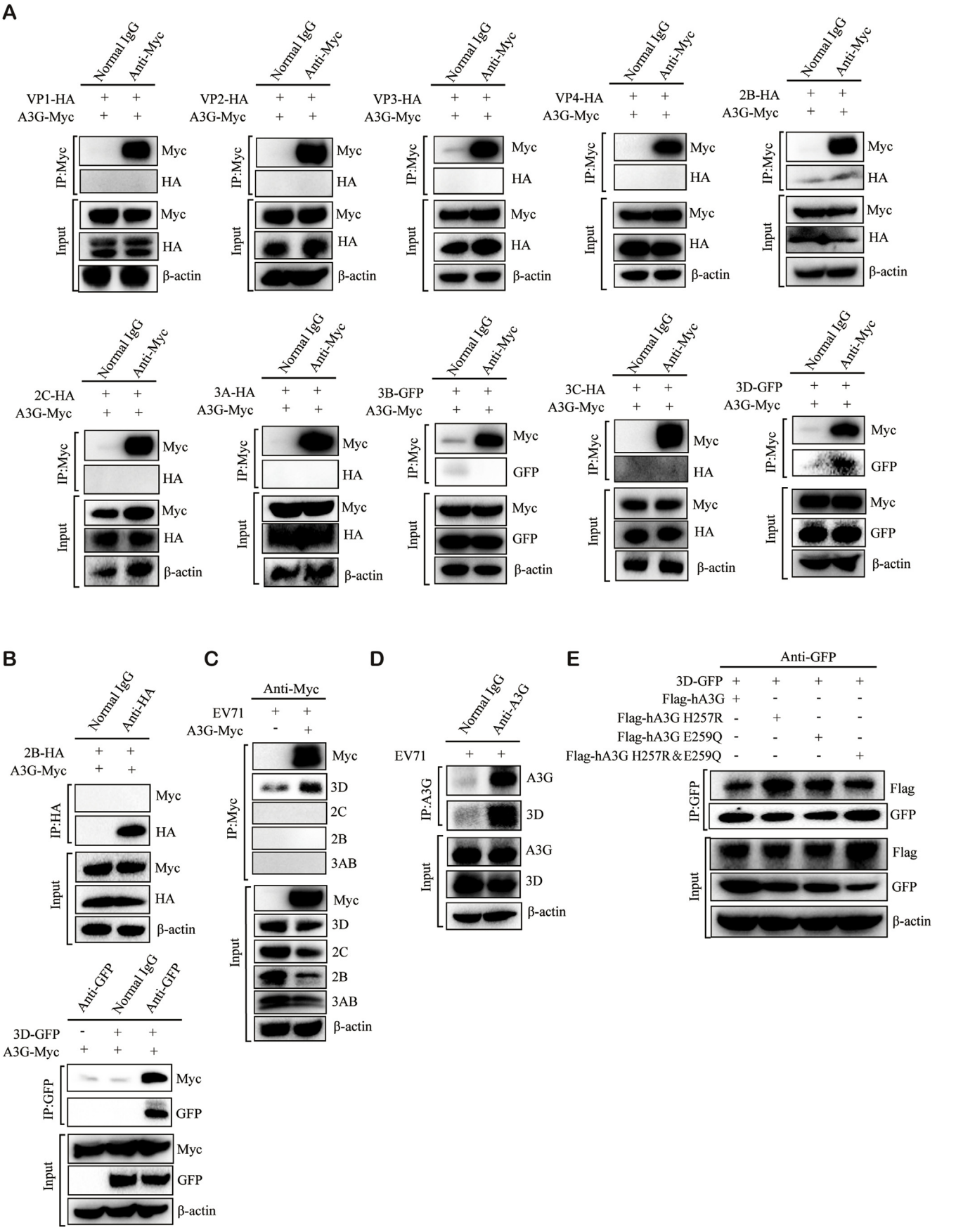

(caption on next page)

Fig. 5. EV71 3D protein specifically interacts with A3G in virally infected cells. (A) 293T cells were co-transfected with a plasmid expressing Myc-A3G and a plasmid expressing HA-VP1, HA-VP2, HA-VP3, HA-VP4, HA-2B, HA-2C, HA-3A, GFP-3B, HA-3C, GFP-3D with Myc-A3G. (B) 293T cells were co-transfected with a plasmid expressing Myc-A3G and a plasmid expressing HA-2B, GFP-3D. (C) 293T cells were transfected with a control vector plasmid or plasmid expressing Myc-A3G, the cells were infected with EV71 at 24 h post transfection and harvested at 24 h post infection. Immunoprecipitation from cell lysates were performed and probed with the indicated antibodies. (D) HCT-8 cells were infected with EV71 and harvested at 24 h post infection. Immunoprecipitation from cell lysates were performed and probed with the indicated antibodies. (E) 293T cells were co-transfected with a plasmid expressing GFP-3D and a plasmid expressing wild-type and indicated mutant Flag-A3G and harvested at 24 h post transfection. Immunoprecipitation from cell lysates was performed and probed with the indicated antibodies.

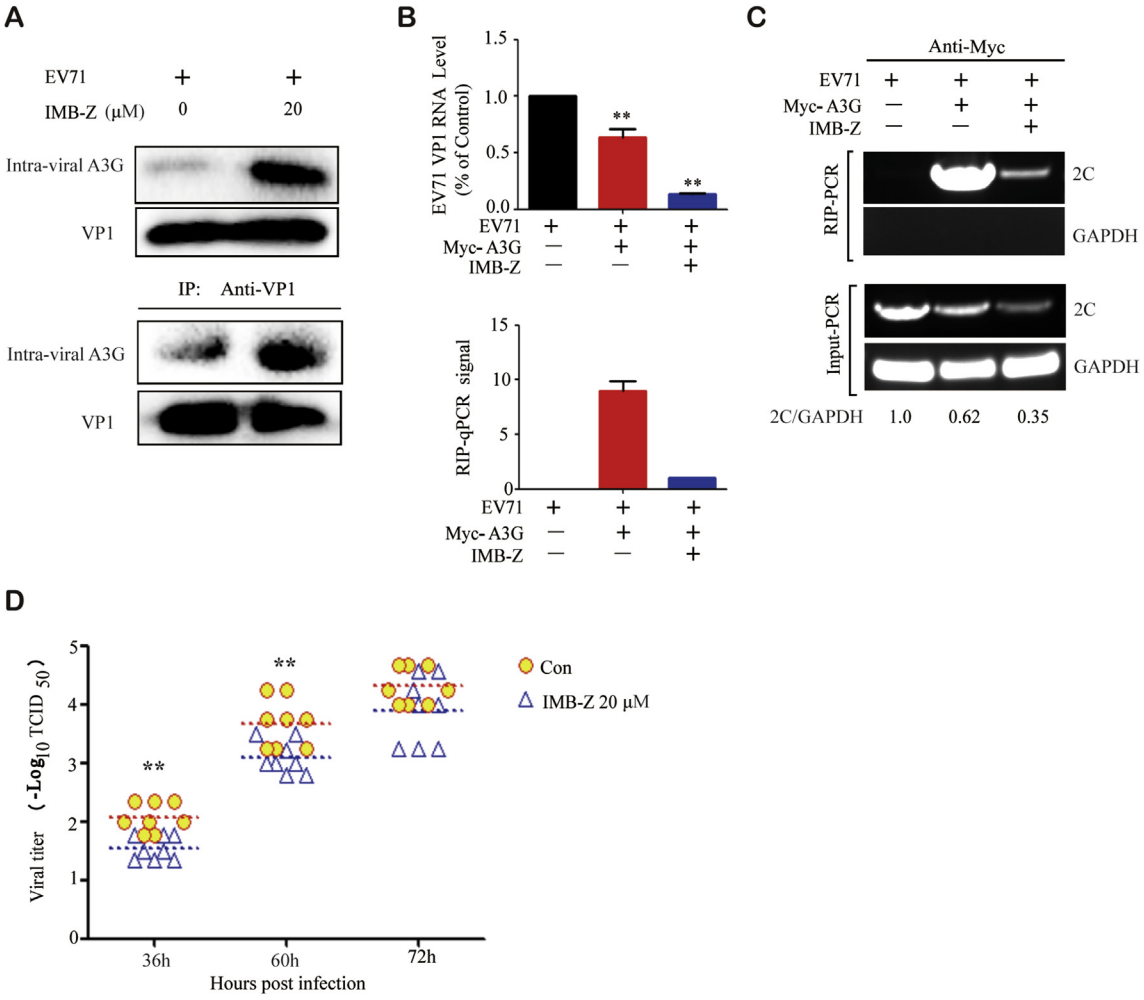

Fig. 6. IMB-Z treatment increases A3G encapsidation into progeny virions and reduces its infectivity. (A) Virion encapsidation of host A3G protein (intraviral A3G) was increased in EV71 particles released from the IMB-Z treated EV71-infected HCT-8 cells. The loading of Western blot assay (upper panel) and import of IP assay (lower panel) were adjusted to equal amount of viral protein VP1. (B, C) Formaldehyde-RIP-qPCR.assay. 293T cells overexpressing Myc-A3G were infected with EV71 and then treated with or without IMB-Z. Cell lysates from formaldehyde treated cells were subjected to IP with an anti-Myc and quantified by qRT-PCR (B) and PCR (C). (D) The $TCID_{50}$ of the progeny viruses generated in HCT-8 cells with or without IMB-Z treatment was determined by CPE assay in Vero cells. The viral titers were measured at the indicated times post infection. $^{**}P < 0.01$.

further demonstrated that IMB-Z inhibits EV71 replication by elevating the intracellular level of A3G and promoting the packaging of A3G into virion particles, which reduces the infectivity of progeny virions.

EV71 infection can lead to a variety of mild or serious illnesses and death (Wang et al., 2012a, 2017; Wu et al., 2013). Although several direct-acting antiviral agents were developed in the last three decades, none of them has been approved, due to limited efficacy or toxicity in clinical trials (Bauer et al., 2017). In addition, the short-term viremia in patients may be also responsible for the failure of antiviral therapy (Cheng et al., 2014). The host-targeting antiviral approach may be useful to combat EV71 infection. Particularly, the short treatment duration may avoid potential toxicity associated with such therapy (Bauer et al., 2017). Although the mechanisms underlying those interesting findings remain to be further investigated, it is rather clear that IMB-Z modulation of A3G metabolism or function is a broad-spectrum antiviral therapeutic approach warranted further investigation.

Ethics approval and consent to participate

Not applicable.

Consent for publication

Not applicable.

Availability of data and material

The datasets supporting the conclusions of this article are included within the article.

Conflicts of interest

The authors have declared that they have no competing interests.

Acknowledgement

We gratefully acknowledge Professor Jutao Guo (Baruch S. Blumberg Institute, PA, USA) for helpful discussions and expert advice on the manuscript.

The work was financially supported by the National Natural Science Foundation of China (81503118) and CAMS Initiative for Innovative Medicine (CAMS-I2M-1-010). This work was also supported by Science Fund for Creative Research Groups of the National Natural Science Foundation of China (81621064) and National Science and Technology Major Projects for “Major New Drugs Innovation and Development” (2018ZX09711003).

Appendix A. Supplementary data

Supplementary data to this article can be found online at https://doi.org/10.1016/j.antiviral.2019.03.005.

References

Albin, J.S., Harris, R.S., 2010. Interactions of host APOBEC3 restriction factors with HIV-1 *in vivo*: implications for therapeutics. Expert Rev. Mol. Med. 12, e4.

Bauer, L., Lyoo, H., van der Schaar, H.M., Strating, J.R., van Kuppeveld, F.J., 2017. Direct-acting antivirals and host-targeting strategies to combat enterovirus infections. Curr. Opin. Virol. 24, 1–8.

Bishop, K.N., Verma, M., Kim, E.Y., Wolinsky, S.M., Malim, M.H., 2008. APOBEC3G inhibits elongation of HIV-1 reverse transcripts. PLoS Pathog. 4, e1000231.

Cardosa, M.J., Perera, D., Brown, B.A., Cheon, D., Chan, H.M., Chan, K.P., Cho, H., Mcminn, P., 2003. Molecular epidemiology of human enterovirus 71 strains and recent outbreaks in the Asia-Pacific region: comparative analysis of the VP1 and VP4 genes. Emerg. Infect. Dis. 9, 461–468.

Cen, S., Peng, Z.G., Li, X.Y., Li, Z.R., Ma, J., Wang, Y.M., Fan, B., You, X.F., Wang, Y.P., Liu, F., Shao, R.G., Zhao, L.X., Yu, L., Jiang, J.D., 2010. Small molecular compounds inhibit HIV-1 replication through specifically stabilizing APOBEC3G. J. Biol. Chem. 285, 16546–16552.

Chelico, L., Pham, P., Petruska, J., Goodman, M.F., 2009. Biochemical basis of immunological and retroviral responses to DNA-targeted cytosine deamination by activation-induced cytidine deaminase and APOBEC3G. J. Biol. Chem. 284, 27761−−27765.

Chen, M., Ju, Y., Chen, M., Xie, Z., Zhou, K., Tan, Y., Mo, J., 2017. Epidemiological and genetic characteristics of EV71 in hand, foot, and mouth disease in Guangxi, southern China, from 2010 to 2015. PLoS One 12, e0188640.

Cheng, H.Y., Huang, Y.C., Yen, T.Y., Hsia, S.H., Hsieh, Y.C., Li, C.C., Chang, L.Y., Huang, L.M., 2014. The correlation between the presence of viremia and clinical severity in patients with enterovirus 71 infection: a multi-center cohort study. BMC Infect. Dis. 14, 417.

Chiu, Y.L., Greene, W.C., 2008. The APOBEC3 cytidine deaminases: an innate defensive network opposing exogenous retroviruses and endogenous retroelements. Annu. Rev. Immunol. 26, 317–353.

Conticello, S.G., Harris, R.S., Neuberger, M.S., 2003. The Vif protein of HIV triggers degradation of the human antiretroviral DNA deaminase APOBEC3G. Curr. Biol. 13, 2009–2013.

Fehrholz, M., Kendl, S., Prifert, C., Weissbrich, B., Lemon, K., Rennick, L., Duprex, P.W., Rima, B.K., Koning, F.A., Holmes, R.K., Malim, M.H., Schneider-Schaulies, J., 2012. The innate antiviral factor APOBEC3G targets replication of measles, mumps and respiratory syncytial viruses. J. Gen. Virol. 93, 565–576.

Goila-Gaur, R., Strebel, K., 2008. HIV-1 Vif, APOBEC, and intrinsic immunity. Retrovirology 5, 51.

He, S.Z., Chen, M.Y., Xu, X.R., Yan, Q., Niu, J.J., Wu, W.H., Su, X.S., Ge, X.S., Zhang, S.Y., Xia, N.S., 2017. Epidemics and aetiology of hand, foot and mouth disease in Xiamen, China, from 2008 to 2015. Epidemiol. Infect. 145, 1865–1874.

Hao, H.J., Hao, S.J., Chen, H.H., Chen, Z., Zhang, Y.F., Wang, J., Wang, H.Z., Zhang, B., Qiu, J.M., Deng, F., Guan, W.X., 2018. N6-methyladenosine modification and METTL3 modulate enterovirus 71 replication. Nucleic Acids Res. https://doi.org/10.1093/nar/gky1007.

Huang, Y.P., Lin, T.L., Kuo, C.Y., Lin, M.W., Yao, C.Y., Liao, H.W., Hsu, L.C., Yang, C.F., Yang, J.Y., Chen, P.J., Wu, H.S., 2008. The circulation of subgenogroups B5 and C5 of enterovirus 71 in Taiwan from 2006 to 2007. Virus Res. 137, 206–212.

Iwatani, Y., Takeuchi, H., Strebel, K., Levin, J.G., 2006. Biochemical activities of highly purified, catalytically active human APOBEC3G: correlation with antiviral effect. J. Virol. 80, 5992–6002.

Jaguva Vasudevan, A.A., Perkovic, M., Bulliard, Y., Cichutek, K., Trono, D., Häussinger, D., Münk, C., 2013. Prototype foamy virus bet impairs the dimerization and cytosolic solubility of human APOBEC3G. J. Virol. 87, 9030–9040.

Ji, X.Y., Wang, H.Q., Hao, L.H., He, W.Y., Gao, R.M., Li, Y.P., Li, Y.H., Jiang, J.D., Li, Z.R., 2013. Synthesis and antiviral activity of N-phenylbenzamide derivatives, a novel class of enterovirus 71 inhibitors. Molecules 18, 3630–3640.

Kitamura, K., Wang, Z., Chowdhury, S., Simadu, M., Koura, M., Muramatsu, M., 2013. Uracil DNA glycosylase counteracts APOBEC3G-induced hypermutation of hepatitis B viral genomes: excision repair of covalently closed circular DNA. PLoS Pathog. 9, e1003361.

Köck, J., Blum, H.E., 2008. Hypermutation of hepatitis B virus genomes by APOBEC3G, APOBEC3C and APOBEC3H. J. Gen. Virol. 89, 1184–1191.

Komohara, Y., Yano, H., Shichijo, S., Shimotohno, K., Itoh, K., Yamada, A., 2006. High expression of APOBEC3G in patients infected with hepatitis C virus. J. Histol. 37, 327–332.

Li, X.Y., Ma, J., Zhang, Q., Zhou, J.M., Yin, X., Zhai, C.J., You, X.F., Yu, L.Y., Guo, F., Zhao, L.X., Li, Z.L., Zeng, Y., Cen, S., 2011. Functional analysis of the two cytidine deaminase domains in APOBEC3G. Virology 414, 130–136.

Li, Z.L., Ning, S.S., Su, X., Liu, X., Wang, H., Liu, Y., Zheng, W.W., Zheng, B.S., Yu, X.F., Zhang, W.Y., 2018. Enterovirus 71 antagonizes the inhibition of the host intrinsic antiviral factor A3G. Nucleic Acids Res. https://doi.org/10.1093/nar/gky840.

Luo, K., Wang, T., Liu, B., Tian, C., Xiao, Z., Kappes, J., Yu, X.F., 2007. Cytidine deaminases APOBEC3G and APOBEC3F interact with human immunodeficiency virus type 1 integrase and inhibit proviral DNA formation. J. Virol. 81, 7238–7248.

Navarro, F., Bollman, B., Chen, H., Konig, R., Yu, Q., Chiles, K., Landau, N.R., 2005. Complementary function of the two catalytic domains of APOBEC3G. Virology 333, 374–386.

Newman, E.N., Holmes, R.K., Craig, H.M., Klein, K.C., Lingappa, J.R., Malim, M.H., Sheehy, A.M., 2005. Antiviral function of APOBEC3G can be dissociated from cytidine deaminase activity. Curr. Biol. 15, 166–170.

Nguyen, D.H., Hu, J., 2008. Reverse transcriptase- and RNA packaging signal-dependent incorporation of APOBEC3G into hepatitis B virus nucleocapsids. J. Virol. 82, 6852–6861.

Noguchi, C., Ishino, H., Tsuge, M., Fujimoto, Y., Imamura, M., Takahashi, S., Chayama, K., 2005. G to A hypermutation of hepatitis B virus. Hepatology 41, 626–633.

Okada, A., Iwatani, Y., 2016. APOBEC3G-Mediated G-to-A hypermutation of the HIV-1 genome: the missing link in antiviral molecular mechanisms. Front. Microbiol. 7, 2027.

Olson, M.E., Harris, R.S., Harki, D.A., 2018. APOBEC enzymes as targets for virus and cancer therapy. Cell Chem. Biol. S2451–9456 (17) 30388-4.

Peng, Z.G., Zhao, Z.Y., Li, Y.P., Wang, Y.P., Hao, L.H., Fan, B., Li, Y.H., Wang, Y.M., Shan, Y.Q., Han, Y.X., Zhu, Y.P., Li, J.R., You, X.F., Li, Z.R., Jiang, J.D., 2011. Host apolipoprotein B messenger RNA-editing enzyme catalytic polypeptide-like 3G is an innate defensive factor and drug target against hepatitis C virus. Hepatology 53, 1080–1089.

Sasada, A., Takaori-Kondo, A., Shirakawa, K., Kobayashi, M., Abudu, A., Hishizawa, M., Imada, K., Tanaka, Y., Uchiyama, T., 2005. APOBEC3G targets human T-cell leukemia virus type 1. Retrovirology 2, 32.

Sheehy, A.M., Gaddis, N.C., Choi, J.D., Malim, M.H., 2002. Isolation of a human gene that inhibits HIV-1 infection and is suppressed by the viral Vif protein. Nature 418, 646–650.

Smith, H.C., Bennett, R.P., Kizilyer, A., McDougall, W.M., Prohaska, K.M., 2012. Functions and regulation of the APOBEC family of proteins. Semin. Cell Dev. Biol. 23, 258–268.

Suspene, R., Guétard, D., Henry, M., Sommer, P., Wain-Hobson, S., Vartanian, J.P., 2005. Extensive editing of both hepatitis B virus DNA strands by APOBEC3 cytidine deaminases in vitro and in vivo. Proc. Natl. Acad. Sci. U.S.A. 102, 8321–8326.

Wang, H.Q., Meng, S., Li, Z.R., Peng, Z.g., Han, Y.X., Guo, S.S., Cui, X.L., Li, Y.H., Jiang, J.D., 2013. The antiviral effect of 7-hydroxyisoflavone against Enterovirus 71 in vitro. J. Asian Nat. Prod. Res. 15, 382–389.

Wang, H.Q., Li, K., Ma, L.l., Wu, S., Hu, J., Yan, H.Y., Jiang, J.D., Li, Y.H., 2017. Berberine inhibits enterovirus 71 replication by downregulating the MEK/ERK signaling pathway and autophagy. Virol. J. 14 2-2.

Wang, X., Zhu, C., Bao, W., Zhao, K., Niu, J., Yu, X.F., Zhang, W., 2012a. Characterization of full-length enterovirus 71 strains from severe and mild disease patients in northeastern China. PLoS One 7, e32405.

Wang, X., Ao, Z., Chen, L., Kobinger, G., Peng, J., Yao, X., 2012b. The cellular antiviral protein APOBEC3G interacts with HIV-1 reverse transcriptase and inhibits its function during viral replication. J. Virol. 86, 3777–3786.

Wu, W.H., Kuo, T.C., Lin, Y.T., Huang, S.W., Liu, H.F., Wang, J., Chen, Y.M., 2013. Molecular epidemiology of enterovirus 71 infection in the central region of Taiwan from 2002 to 2012. PLoS One 8, e83711.

Zhu, Y.P., Peng, Z.G., Wu, Z.Y., Li, J.R., Shuang, M.H., Si, S.Y., Jiang, J.D., 2015. Host APOBEC3G protein inhibits HCV replication through direct binding at NS3. PLoS One 10, e0121608.